ANTS with Firefly Communication

Chin A. Lua
Department of Computer Science & Operations Research
North Dakota State University
Fargo, ND 58105, USA

Karl Altenburg
Department of Accounting and Information Systems
North Dakota State University
Fargo, ND 58105, USA

Kendall E. Nygard
Department of Computer Science & Operations Research
North Dakota State University
Fargo, ND 58105, USA

Abstract — Autonomous Nano-Technology Swarm (ANTS) from NASA employs numerous, autonomous, l-kg solar sails for surveying and studying asteroids in the Asteroid Belt. There is no convincing work on a simulator that validates the solar sail's behaviors and weak propellant system in the extreme space environment. Thus, we have developed and verified an Environment Agent (EA) that simulates gravity and light force based on well-understood Newtonian and sound light force equations. Sail Agents (SA) simulate swarm behaviors that are able to turn their reflective surface in four orthogonal directions and produce 3-D maneuvers. The simulator is able to convincingly model key behaviors of SAs. We also provide a model that has the simplest swarm behaviors and unorthodox sensors for testing feasibility of ANTS using EA. The communication is done via on-off light patterns – firefly.

Keywords — Environment Agent, Firefly-like Communication, Sail Agent.

1.0 Introduction

The main goal of Autonomous Nano-Technology Swarm (ANTS) is to employ systems of up to 1000 autonomous solar sails with l-kg mass each for surveying and studying asteroids in the Asteroid Belt around the year 2025 [2, 18, 19, 20, 21]. The propellant system uses the force created by light photons striking on the thin, reflective sail surface. This light force is only $9.12 * 10^{-6}$ N/m^2 (1 N=1 kg * 1 m/s^2) at 1 Astronomical Unit (AU) [1, 4]. ANTS is among very few NASA projects that employ swarm behaviors.

The authors have studied swarm behaviors for the U.S. Air Force and Navy [9, 10, 11] in Unpiloted Air Vehicle (UAV) applications. We view the required swarm behaviors are similar but note the following differences between ANTS and UAV: 1) the UAV's forces are well understood and ample experimental data are available, 2) the UAV's engine is much more powerful and flexible in maneuvering, and 3) a UAV is much heavier than 1 kg and thus has fewer restrictions on navigation sensors and communication.

Since ANTS is a novel concept, basic feasibility questions arise. E.g., for a 1-kg sail with 100 m^2 reflective surface, the light force is $9.12 * 10^{-4}$ N ($9.12 * 10^{-6}$ N/m^2 * 100 m^2) at 1 AU. The acceleration generated by this force is $9.12 * 10^{-4}$ m/s^2. At 3.3 AU, it is $8.37 * 10^{-5}$ m/s^2 ($9.12 * 10^{-4}$/ (3.3 * 3.3)). Therefore, it is of interest to understand what *useful* swarm behaviors are feasible under such conditions.

We devised a simple and accurate simulator to provide answers to key feasibility questions. This simulator must simulate the gravity and light force everywhere within a discrete time step chosen (i.e., one second) and provide numerical values and animations that verify swarm behaviors.

2.0 Related Work

There is little work pertaining to spacecrafts propelled by light force. The available literature concentrates on theoretical mathematical formulae about light force [3, 8]. However, mathematics cannot describe the gravitational effects for more than three bodies, independent of the role of light force. This classical n-body problem can only be addressed by simulation. In addition, for emergent swarm behaviors, we rely heavily on a simulator that can reveal the global effects resulted from local heuristics exercised by individual swarm members. To the best of our knowledge, there is no convincing work on a simulator that validates the solar sail's behaviors and propellant system in an extreme space environment. The development of such a simulator is our basic contribution.

3.0 ANTS Simulator

The simulator consists of the EA and SA parts. The EA component simulates the gravity and light force in the solar system at each location and second. The SA component simulates the behaviors that are responsible for turning the reflective surface of the sail. EA will not be part of a real sail, but SA will. EA serves in the simulator to enforce physical laws over all behaviors, including non-swarm behaviors or algorithms.

Gravity and light force are approximated (thus, errors) via vectors and assumed to be constant throughout the second. The *accumulated error* in each second is passed to the next. We prove that this error is so small that it does not significantly affect the accuracy of the force vector calculations described in section 4.0.

At the *beginning* of each simulated second, EA calculates: 1) the change of acceleration as a consequence of the forces of gravity and light acting upon a sail, 2) the change of the sail's velocity resulting from acceleration, and 3) the change of the sail's position (displacement) caused by the velocity. EA will move the sail to that position at the end of the second, and the steps are then repeated for the next second. SA cannot affect the gravity in any way; but nevertheless, can control the light force by turning its surface in four orthogonal directions.

EA is the basic model for testing the feasibility of ANTS system. The following simplifications are assumed for EA: 1) Newton's mechanics and Galileo's relativity are employed since they are simple and sufficiently accurate for the simulations, 2) a second is constant everywhere in the space as described by Galileo's relativity, 3) modeling the large gravity of the sun, but ignoring all other planets, and 4) the sail can still receive the light force when a small object is blocking part of the rays of the sun.

The force-vector calculations in EA are validated through a mathematical induction argument: 1) there are n equal simulated seconds, 2) the net acceleration, velocity, and displacement can be verified for the first second (i.e., for n=1), 3) the mechanism is the same in each second (i.e., the shape of any n and n+1 seconds is the same), 4) second n+1 continues the results from second n, and 5) by mathematical induction the simulated result is valid for each n (n is finite).

4.0 Gravity in EA

4.1 The Design

Gravity is a major component of EA that we develop in detail from the bottom up to provide validation in three ways: 1) the universal gravity equations implemented in coding are validated to ensure that they provide the intended results, 2) the simulated results meet accuracy standards, and 3) the underlying force-vector model is sound.

The three properties can be proven via the validity of the Newtonian universal equations (1), (2), & (3) stated below. Equation (1) and (2) describe gravity everywhere, including a perfect circular orbit, but equation (3) describes gravity specifically that results in a perfect circular orbit. Theoretically, with the same initial values, both groups of equations describe the same orbit. We based our code on equation (1) and (2), *but not equation (3)*. We demonstrate the three validations by establishing that our computational results have high fidelity to a theoretical perfect circular orbit.

Gravity from the sun acting upon the sail is computed using Newton's gravitational law:

$$\text{Gravity} = GMm/r^2$$

$$\textit{Gravity} = GM/r^2 \qquad (1)$$

Where G = constant of gravitation

$= 6.6742 * 10^{-11}\ m^3\ kg^{-1}s^{-2}$ [6]

M = sun's mass = $1.9891 * 10^{30}$ kg [5]

m = sail's mass = 1 kg

r = distance between sail and sun

Equation (1) is simple to use since the only variable is r. Once the gravity is known, the acceleration is given by Newton's second law:

$$F = ma$$

Where F = sun's attractive force on sail

m = sail's mass = 1 kg

a = sail's acceleration

Since the sail's mass = 1 kg, the equation can be simplified:

$$F = a \qquad (2)$$

If the acceleration is known, the change of the sail's velocity and position within a given second can be calculated. For example, the sail's acceleration at 1 AU, 149597870000 meters [5], from the sun is computed as:

(2) = (1), by Galileo's Principle of Equivalence

$$a = GM/r^2$$

$$a = 6.6742 * 10^{-11} m^3 kg^{-1} s^{-2} * 1.9891 * 10^{30}\ kg / (149597870000\ m)^2$$

$$a = 5.9321 * 10^{-3}\ m/s^2$$

Since the acceleration *a* is a vector, one cannot determine the change of velocity and displacement without its direction. Some possible directions of sail's starting acceleration, velocity, and displacement are depicted in the left of Fig. 1

below. 5.9321 * 10^{-3} m/s^2 means the change of velocity in 1 second is 5.9321 * 10^{-3} m/s (Newton's 2nd Law) in vector *a*'s direction. If we assume velocity *v*'s magnitude is 0.018 m/s and 90 degrees (for this case only) from acceleration *a*, then the net velocity, *u*, is computed by vector addition shown in the right of Fig. 1:

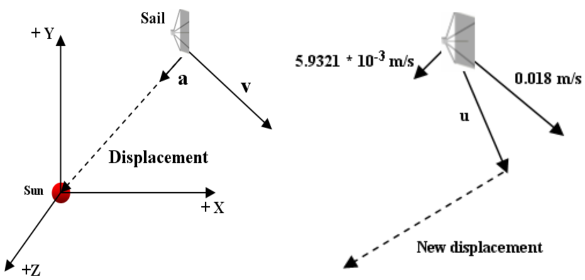

Fig. 1. Sail's vectors in Java 3D

The vector *u*'s magnitude is the square root of (5.9321 * 10^{-3} m/s)^2 + (0.018 m/s)^2, which is 1.8952 * 10^{-2} m/s in velocity *u*'s direction. The new displacement represents the new sail's location at the end of the second. The process is repeated again for the next second. Note that equation (3) is not involved.

Newton's second law can also be applied in circular motion:

$$ma = mv^2/r$$
$$a = v^2/r \qquad (3)$$

Where *v* is velocity and the other factors are defined above. Equation (3) is well tested through experiments. It indicates that for a perfect circular orbit, *r* is constant since it is the radius of the perfect circle. If *r* is constant, then acceleration *a* must be constant (since this is the same force at equal distance and thus the same acceleration, equation (1) & (2)), and by the validity of equation (3), the magnitude of velocity *v* is constant, as well too. The direction of velocity *v* is a tangent to the circle since any other directions will either increase or decrease the magnitude of the velocity.

4.2 Empirical Observation and Experiments

Animations were developed and numerical data used available for gravity verification. At the start of the simulation, EA positions the sail at coordinate (149597870000, 0, 0). That is, 1 AU at the X-axis from the origin (0, 0, 0). Since we need to show that EA pushes the sail around a *near* perfect circular orbit, equation (3) is used to calculate the *theoretical starting velocity (i.e., at time = 0 second only)* at 1 AU for the sail, which is 2.9789 * 10^4 m/s. We noted visually that the sail moved in a circle. With regard to numerical data, the speeds and radii of the sail at 1 AU confirm the same observation. Table 1 shows 10 speeds and radii (from sail to sun) at the n^{th} second. Unlike the theoretical starting values, the n^{th}-second speed and radius are *accumulated approximations* calculated from equation (1) & (2) by EA.

Table 1. Sail's orbiting seconds, speeds, and radii at 1 AU.

*Theoritical starting speed for sail = 2.9789 * 10^4 m/s*
Theoritical starting radius from sail to sun = 149597870000 m

Orbiting Time (n^{th} second)	n^{th}-second speed - *starting speed* (m/s)	n^{th}-second radius - *starting radius* (m)
3155296	**1.7434 * 10^{-3}**	**-8.7549 * 10^3**
6310592	**2.8209 * 10^{-3}**	**-1.4166 * 10^4**
9465888	**2.8209 * 10^{-3}**	**-1.4166 * 10^4**
12621184	**1.7434 * 10^{-3}**	**-8.7549 * 10^3**
15776480	**-7.3487 * 10^{-9}**	**7.1442 * 10^{-2}**
18931776	**-1.7434 * 10^{-3}**	**8.7550 * 10^3**
22087072	**-2.8209 * 10^{-3}**	**1.4166 * 10^4**
25242368	**-2.8209 * 10^{-3}**	**1.4166 * 10^4**
28397664	**-1.7434 * 10^{-3}**	**8.7550 * 10^3**
31552960	**-5.3878 * 10^{-9}**	**8.4320 * 10^{-2}**

From Table 1, the *accumulated* speeds and radii are nearly constant throughout the simulated seconds. For example, the difference between the 31552960th-second (about 1 year) and theoretical starting speed is -5.3878 * 10^{-9} m/s. Similarly, the difference in radius is 8.4320 * 10^{-2} m. Over simulation runs of hours, the differences in speed and radius at the 6.988 * 10^{10th} second (2215 years) were -2.7537 * 10^{-3} m/s and 1.3828 * 10^4 m. Other numerical data at other locations such as 3.3 AU confirm the same observations of Table 1. Thus, the sail travels in a *near* perfect circle *as predicted* in our design in section 4.1. This establishes the three validations.

5.0 Gravity and Light Force in EA

5.1 The Model Design

After validating the underlying force-vector model, the next step is to add light force vectors to the proven model. Blomquist's equations [3] are employed since the light force equations are in vector forms. The equations are as follow:

$$\text{drag} = 9.12 * 10^{-6} * s\,(f_r \cos^3\theta + 1/2\,(1 - f_r)\cos\theta)$$
$$\text{lift} = 9.12 * 10^{-6} * s\,(f_r \cos^2\theta \sin\theta)$$

Where θ = the angle between incident light & sail surface's normal.
s = total sail's surface in square meters.
9.12 * 10^{-6} N/m^2 = light force/m^2 due to normal incident light (i.e., θ = 0) at 1 AU.
lift = a force component along orbit.

drag = a force component away from sun.
f_r = sail material's reflectivity, 1 means all reflected, and 0 means all absorbed.

Graphically, they are depicted in Fig. 2:

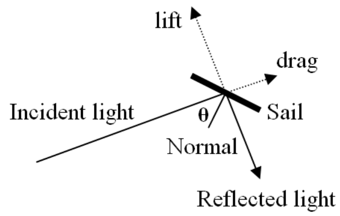

Fig. 2. Light force components.

From Fig. 2, drag is the force vector that is in the direction of incident light, where lift is the force vector that is perpendicular to the incident light. The light force equations are formulated at 1 AU only. We modify them into universal equations for any sail that is r meters away from the sun with 100 m^2 sail surface as:

$$drag = 9.12 * 10^{-4} (AU/r)^2 (f_r \cos^3\theta + 1/2 (1 - f_r) \cos \theta) \quad (4)$$

$$Lift = 9.12 * 10^{-4} (AU/r)^2 (f_r \cos^2 \theta \sin \theta) \quad (5)$$

A few observations about equation (4) & (5) are noted here. First, since the sail's mass is 1 kg, the light force vectors in the equations are equal to their respective accelerations using equation (2). Second, θ describes how the sail turns its surface. Third, if $\theta = 90^o$, both drag and lift becomes 0 and thus has no light force – this means the edge of solar sail's surface is facing the sun directly. Fourth, if $\theta = 0^o$ & $f_r = 1$, then lift = 0, but drag = $9.12*10^{-4}$ m/s^2 [1, 4] – this implies that the sail's entire reflective surface is facing the sun directly. Fifth, if $\theta = 35.3^o$ & $f_r = 1$, lift has maximum value of $3.51 * 10^{-4}$ m/s^2. Sixth, for light force simulations, we assume $f_r = 1$ for all θ. Finally, all lifts have drag counterparts, which imply that a sail moving in a circular orbit around an asteroid (one of the main goals of ANTS) could be difficult, if not impossible, as none of the drags or lifts are pointing towards the sun.

The light force calculations are similar to the gravity example above except for their directions. Nevertheless, the following points should be mentioned: 1) the *proven* acceleration *a* is always orthogonal to *lift* but parallel and opposite to *drag*, 2) Java 3D will compute the net force by vector addition of *a*, *lift*, and *drag*, 3) the net acceleration will change the sail's velocity *v*, 4) the changed velocity *v* will change the *displacement* at the end of the second, and 5) the process is repeated in the next second.

SA can turn its surface counterclockwise (CC), clockwise (CW), up, and down as shown in Fig. 3.

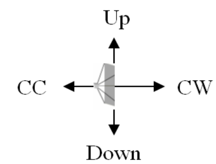

Fig. 3. Four ways in turning sail's surface

CC is turning the cross counterclockwise horizontally with Up-Down arrows fixed. The opposite is CW. Up is turning the cross clockwise vertically with CC-CW arrows fixed. The opposite is Down. SA can only choose one of the four turnings in each second. Without them, the sail cannot move in a 3-D space. Equation (4) & (5) can repeatedly be applied in each direction as we have intentionally designed the surface as a square. Unlike the gravity design, there is no other well-established theoretical universal light force equations to prove the validity of equation (4) & (5) in coding. However, if the equations are incorrect (not likely), we could potentially replace them with others as the underlying model in EA is still sound.

5.2 Empirical Observation and Experiment

One way to verify light force without well-established theoretical universal equations is to compare its behaviors against those proven ones from gravity. Thus, an asteroid ball (that obeys gravity only) and a sail (that obeys both gravity and light force) are available for animations and numerical analysis. At the beginning of the simulation, both objects will start together at the same location and velocity. With a default $\theta = 90^o$, they move out together in the same circular orbit as described in section 4.0 until the user changes the θ value from GUI.

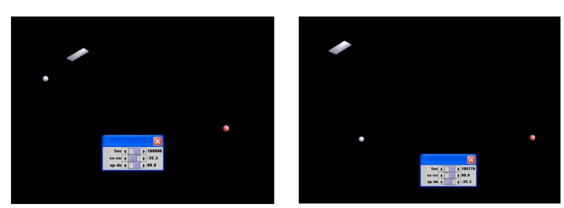

Fig. 4. Light force reduces (left) or increase (right) sail's velocity

In Fig. 4, the left picture shows that the sail's speed is slower than the ball by setting $\theta=-35.3^o$. The opposite setting will increase the speed as depicted in the right picture. We have visually confirmed that the sail was able to *maneuver in 3-D space* using the four turnings *manually*, even at 3.3 AU. We analyzed the numerical data and the values agree with equation (4) & (5). However, it was difficult to make the sail closed to the ball via SA by using the four turnings *manually*. Hence, the initial results indicate that it may not be possible to have useful maneuvers around the asteroid, which is basic experimental contribution of our work.

In summary, we established that the light vectors are sound because: 1) the underlying light vector calculations are based upon mathematical induction as explained in section 3.0, 2) the much weaker light vectors are added to the validated gravity vectors, 3) the observed light force effects in the simulator were consistent, 4) all vector calculations were monitored in one short Java method, and 5) we used Java 3D methods like vector1.angle (vector2) to check the orthogonality of gravity, lift, and drag in each calculation; thus, we are assured that the direction (which is more useful than magnitude) of each vector is correct.

6.0 SA

It will be a waste of effort and time in developing higher-level and complex swarm behaviors if there is evidence that some of ANTS' *useful* maneuvers, like orbiting around an asteroid, are in doubt. Hence, we designed a simple, reactive model that consists of avoid and attract behaviors for SA to see whether the sails can form a group. Grouping is crucial in ANTS, and if EA fails it, ANTS project will not be feasible. To design a practical swarm application, we need to consider the constraints imposed by the navigation sensors. Unfortunately, the sensors today weight much more than 1 kg and threaten the survival of ANTS. Thus, we need to consider unorthodox sensors and the protocols for using them. This model is inspired by fireflies that use light patterns to pass messages to each other when they group together at night. Light is abundant in the solar system. If we can use light effectively in our designs, it would minimize the required sensor weight.

6.1 ANTS with Firefly Scenarios

The scenarios for the firefly model are described below:

- A group of sails and an asteroid ball start out together. The ball's only behavior is to orbit the sun. The sail will use light to communicate with other sails and determine their distances by estimating the calibrated light intensity.
- They will follow a protocol in flashing their communication lights.
- The sail will be attracted to each other or the ball when they are in "attraction" zone; but will repelled by each other or the ball when they are in a "close" zone.
- Each sail will choose the closest neighbor to attract or repel.
- Each sail will select a random sail orientation and tack to move.
- The agent will be rewarded for a sail orientation and tack that has the desired result and continue to use that configuration; if it does not have the intended effect, the agent will choose another configuration at random.
- The sail does not know its velocity and does not have access to a centralized, shared clock.

6.2 SA's Sensors

Four simple, unorthodox navigation sensors are proposed for basic navigation.

1. Sun sensor – the sensor could be a charge coupled device (CCD) such as those used in digital cameras. A CCD-based sensor is chosen because: 1) it is very sensitive – able to detect single photons [7], 2) it is lightweight and small, 3) it can measure the incident angle of incoming light, and 4) it requires little power. The CCD-based sensors can be further developed to provide sails for the following navigation functions: 1) to provide a sun line as a reference in turning the sail's surface, 2) to provide an estimate distance from the sun based on calibration and the inverse-square law, and 3) to measure distances from other nearby sails by estimating calibrated light intensity emitted from other sails.

2. LEDs for light communication – sails could use light patterns generated by high-intensity LEDs for communication. LEDs are used because they can efficiently generate bright light, and the technology is already used extensively and more efficient products are in development. LEDs can be used by solar sails to transmit simple messages. A light-flashing protocol is needed for cooperation and execution of scalable swarm behaviors: 1) if a solar sail transmits first, the others will stop and observe the message, 2) the others will take note of the message if it concerns them, 3) if the message

concerns them, they will give up their option to transmit, 4) nevertheless, they will answer a service requested by the requesting agent, and 5) once the sail stops transmitting, the others will contend to transmit next.

3. Cameras – all solar sails are basically "blind." However, they can build a relative frame of reference using cameras. E.g., once the sun sensor has determined the sun line, the sail can build the XYZ-coordinate system that records the relative positions of the sun, sails, and other objects. Sails cannot estimate distances from dark objects like asteroids since the reflected light is not calibrated like LED or sun light. Thus, the sails need a new way to estimate the distance to an asteroid or other dark objects. We suggest a sensor that consists of two movable cameras mounted and fixed on a movable board to determine the distances of asteroids and dark objects.

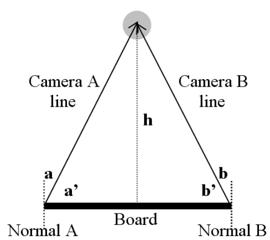

Fig. 5. Movable cameras and board

Two cameras in Fig. 5 are placed at both edges of the board. When the asteroid's image is visible, both camera A and B will capture it at their view centers as shown by the respective camera lines. Angle a and b are calculated each time the cameras change their camera lines relative to the normals. The cameras communicate with each other to ensure angle a = angle b. If not, both cameras and the board will move until they are equal. If a = b, then a' = b'. The line h, the distance from the sail to asteroid, can be determined by the trigonometry of isosceles triangle. The accuracy of h depends on: 1) a common algorithm that enables both cameras to spot the same location on the asteroid, 2) the ability of the cameras to repeat the same process above precisely as angle a & b approach to 0, and 3) the length of the board.

4. High speed camera shutters for mass communication. For example, once the worker sails have finished surveying the asteroid with their special sensor, the large data must be passed to a messenger sail that will travel back to earth. LEDs are limited for this function. We propose that light, durable, high-speed shutter rows be placed at the back of a control box where its front end allows sun rays to pass through when necessary. During mass transmission, the messenger sail will use its camera to observe the worker sail's shutters' light patterns created by opening and closing the shutters rapidly. E.g., if each shutter can open or close 10,000 times/second and there are 64 shutters, the worker sail can pass 640,000 bits of information per second to messenger sail.

6.3 SA's basic Behaviors

Two behaviors, attraction and avoidance are enough for sails to form a group. A sail classifies two spheres as close or attraction with critical or safe vision range, respectively. The sail will avoid *the* closest neighbor in close sphere but attract to *the* closest neighbor in attraction sphere. The avoidance has a higher priority than attraction. The authors have implemented these two behaviors successfully on UAVs in future work of [10], which are able to group and move autonomously at a safe distance of each other despite the fact that only the *closest neighbors* are considered.

7.0 SA's Architecture

SA's control structure utilizes a decentralized behavior-based architecture inspired by the subsumption architecture [12], motor schema [13], [14], and force fields [15], [16], [17]. The two basic behaviors in this architecture are shown in Fig. 6.

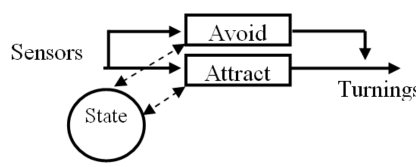

Fig. 6. Control structure.

At each simulated second, the control architecture reads both the external *sensors and internal state* to invoke the appropriate behavior by which a sail's turning is set. If there is no input from the state, the higher behavior layer will inhibit and subsume the lower layer(s) as required by the subsumption scheme. The behavior layers will grow vertically as more behaviors are added. The original Brook's subsumption scheme does not have an internal state. We added it for practical, purposeful swarm applications based on our experience. For example, the state, which always has the highest priority than sensors, can ask SA to self-destruct by choosing only attract behavior with the *goal* of colliding with other objects. Nonetheless, we view the tight coupling between the sensors and state and behaviors is still responsible for SA's reactive maneuvers as in [10] that implements the same architecture. The pure subsumption may consider the state as a monolithic internal control that will hamper the emergence of intelligence.

8.0 Future Work

There is considerable future work for ANTS: 1) the authors would like to add more objects to EA, 2) the firefly agent model should be coded and tested by EA, 3) synchronized orbiting behavior around an asteroid needs to be tested by EA, and 4) higher and complex behaviors will be introduced and tested by EA once the basic maneuvers are established.

9.0 Conclusion

We believe that we have laid a solid foundation for solving this problem. We conclude the relative importance of the concepts we have established in the following implications: no proven gravity vectors imply no light force vectors imply no EA implies no SA implies no solution to the ANTS problem.

10.0 Acknowledgment

This work was sponsored in part by the North Dakota Space Grant Consortium. The authors would like to acknowledge the members of the Orion research group at North Dakota State University for their discussion and insight on this project.

11.0 References

[1] D. Spieth and R. Zubrin, Ultra-Thin Solar Sails for Interstellar Travel: Phase I Final Report, by Pioneer Astronautics, Inc., Lakewood, CA., published December 1999.

[2] Curtis, S.A., J. Mica, J. Nuth, G. Marr, M. Rilee, and M. Bhat, ANTS (Autonomous Nano-Technology Swarm): An Artificial Intelligence Approach to Asteroid Belt Resource Exploration, International Astronautical Federation, 51st Congress, 2000.

[3] R. Blomquist, Solar Blade Nanosatellite Development: Heliogyro Deployment, Dynamics, and Control, Proceedings of the 13th USU / AIAA Small Satellite Conference, 1999.

[4] Jonathan T. Black, Jack Leifer, Joshua A. DeMoss , Eric N. Walker and W. Kevin Belvin, Experimental and Numerical Correlation of Gravity Sag in Solar Sail Quality Membranes, 45th AIAA/ASME/ASCE/AHS/ASC Structures, Structural Dynamics and Materials Conference, AIAA 2004-1579, pp. 9, 2004.

[5] Appendix 2: Basic Constants, Astronomical Reference Material, Astronomy Department, Sierra College. http://astronomy.sierra.cc.ca.us/.

[6] CODATA Internationally Recommended Values of the Fundamental Physical Constants, The NIST Reference on Constants, Units, and Uncertainty. http://physics.nist.gov/.

[7] Chapter 12: Science Instruments, Section II, Basics of Space Flight, Jet Propulsion Laboratory, Caltech. http://www2.jpl.nasa.gov/basics/.

[8] Morrow, E., Scheeres, D.J., Lubin, D., Solar Sail Orbit Operations at Asteroids, AIAA 2000-4420, 2000.

[9] K. Altenburg, J. Schlecht, and K.E. Nygard, An Agent-based Simulation for Modeling Intelligent Munitions, Proceedings of the WSEAS Conference, Greece, 2002.

[10] Chin A. Lua, Karl Altenburg, Kendall E. Nygard, Synchonized Multi-Point Attack by Autonomous Reactive Vehicles with Simple Local Communication, IEEE Swarm Intelligence Symposium, 2003.

[11] Joseph Schlecht, Karl Altenburg, Benzir M. Ahmed, and Kendall E. Nygard, Decentralized Search by Unmanned Air Vehicles using Local Communication, Proceeding of the International Conference on Artificial Intelligence, 2003.

[12] R.A. Brooks, "A Layered Control System for a Mobile Robot," IEEE Journal of Robotics and Automation, Vol. 2:1, pp. 14-23, 1986.

[13] M.A. Arbib, Perceptual Structures and Distributed Motor Control, in Handbook of Physiology, Section 2: The Nervous System, Vol. II, Motor Control, Part 1 (V.B. Brooks, Ed.), American Physiological Society, pp. 1449-1480, 1981.

[14] R.C. Arkin, "Motor Schema-based Mobile Robot Navigation," The International Journal of Robotics Research, pp. 92-112, August 1989.

[15] J.R. Andrews, and N. Hogan, Impedance Control as a Framework for Implementing Obstacle Avoidance in a Manipulator, in David E. Hardt and Wayne J. Book, editors, Control Of Manufacturing Processes and Robotic Systems, ASME, Boston, pp. 243-251, 1983.

[16] O. Khatib, "Real-time Obstacle Avoidance for Manipulators and Mobile Robots," The International Journal of Robotics Research, Vol. 5:1, 1986.

[17] B.H. Krogh, "A Generalized Potential Field Approach to Obstacle Avoidance Control," International Robotics Research Conference, Bethlehem, Pennsylvania, August 1984.

[18] S.A. Curtis, M.L. Rilee, P.E. Clark, and G.C. Marr, Use of Swarm Intelligence in Spacecraft Constellations for the Resource Exploration of the Asteroid Belt, Third International Workshop on Satelllite Constellations and Formation Flying, 2003.

[19] Curtis, S.A., W.F. Truszkowski, M.L. Rilee, and P.E. Clark, ANTS for the Human Exploration and Development of Space, Proceedings of IEEE Aerospace Conference, 2003.

[20] Clark, P.E., Curtis, S.A., Rilee, M.L., Truszkowski, W., Marr, G., Cheung, C.Y., and Rudisill, M., BEES for ANTS: Space Mission Applications for the Autonomous NanoTechnology Swarm, AIAA Intelligent Systems Technical Conference, 2004a.

[21] Clark, P.E., Rilee, M.L., Curtis, S.A., Cheung, C.Y., Marr, G., Truszkowski, W., Rudisill, M., PAM: Biologically inspired engineering and exploration mission concept, components, and requirements for asteroid population survey, IAC Proceedings, 2004c.